

S. Smys

João Manuel R. S. Tavares

Valentina Emilia Balas *Editors*

Computational Vision and Bio-Inspired Computing

Proceedings of ICCVBIC 2021



Springer

Advances in Intelligent Systems and Computing

Volume 1420

Series Editor

Janusz Kacprzyk, Systems Research Institute, Polish Academy of Sciences,
Warsaw, Poland

Advisory Editors

Nikhil R. Pal, Indian Statistical Institute, Kolkata, India

Rafael Bello Perez, Faculty of Mathematics, Physics and Computing,
Universidad Central de Las Villas, Santa Clara, Cuba

Emilio S. Corchado, University of Salamanca, Salamanca, Spain

Hani Hagra, School of Computer Science and Electronic Engineering,
University of Essex, Colchester, UK

László T. Kóczy, Department of Automation, Széchenyi István University,
Gyor, Hungary


Vladik Kreinovich, Department of Computer Science, University of Texas
at El Paso, El Paso, TX, USA

Chin-Teng Lin, Department of Electrical Engineering, National Chiao
Tung University, Hsinchu, Taiwan

Jie Lu, Faculty of Engineering and Information Technology,
University of Technology Sydney, Sydney, NSW, Australia

Patricia Melin, Graduate Program of Computer Science, Tijuana Institute
of Technology, Tijuana, Mexico

Nadia Nedjah, Department of Electronics Engineering, University of Rio de
Janeiro, Rio de Janeiro, Brazil

Ngoc Thanh Nguyen , Faculty of Computer Science and Management,
Wrocław University of Technology, Wrocław, Poland

Jun Wang, Department of Mechanical and Automation Engineering,
The Chinese University of Hong Kong, Shatin, Hong Kong

The series “Advances in Intelligent Systems and Computing” contains publications on theory, applications, and design methods of Intelligent Systems and Intelligent Computing. Virtually all disciplines such as engineering, natural sciences, computer and information science, ICT, economics, business, e-commerce, environment, healthcare, life science are covered. The list of topics spans all the areas of modern intelligent systems and computing such as: computational intelligence, soft computing including neural networks, fuzzy systems, evolutionary computing and the fusion of these paradigms, social intelligence, ambient intelligence, computational neuroscience, artificial life, virtual worlds and society, cognitive science and systems, Perception and Vision, DNA and immune based systems, self-organizing and adaptive systems, e-Learning and teaching, human-centered and human-centric computing, recommender systems, intelligent control, robotics and mechatronics including human-machine teaming, knowledge-based paradigms, learning paradigms, machine ethics, intelligent data analysis, knowledge management, intelligent agents, intelligent decision making and support, intelligent network security, trust management, interactive entertainment, Web intelligence and multimedia.

The publications within “Advances in Intelligent Systems and Computing” are primarily proceedings of important conferences, symposia and congresses. They cover significant recent developments in the field, both of a foundational and applicable character. An important characteristic feature of the series is the short publication time and world-wide distribution. This permits a rapid and broad dissemination of research results.

Indexed by DBLP, INSPEC, WTI Frankfurt eG, zbMATH, Japanese Science and Technology Agency (JST).

All books published in the series are submitted for consideration in Web of Science.

For proposals from Asia please contact Aninda Bose (aninda.bose@springer.com).

More information about this series at <https://link.springer.com/bookseries/11156>

S. Smys · João Manuel R. S. Tavares ·
Valentina Emilia Balas
Editors


Computational Vision and Bio-Inspired Computing


Proceedings of ICCVBIC 2021

 Springer

Editors

S. Smys
Department of ECE
RVS Technical Campus
Coimbatore, Tamil Nadu, India

Valentina Emilia Balas 
Faculty of Engineering
Aurel Vlaicu University of Arad
Arad, Romania

João Manuel R. S. Tavares 
Departamento de Engenharia Mecânica
Faculdade de Engenharia
Universidade do Porto
Porto, Portugal

ISSN 2194-5357

ISSN 2194-5365 (electronic)

Advances in Intelligent Systems and Computing

ISBN 978-981-16-9572-8

ISBN 978-981-16-9573-5 (eBook)

<https://doi.org/10.1007/978-981-16-9573-5>

© The Editor(s) (if applicable) and The Author(s), under exclusive license to Springer Nature Singapore Pte Ltd. 2022

This work is subject to copyright. All rights are solely and exclusively licensed by the Publisher, whether the whole or part of the material is concerned, specifically the rights of translation, reprinting, reuse of illustrations, recitation, broadcasting, reproduction on microfilms or in any other physical way, and transmission or information storage and retrieval, electronic adaptation, computer software, or by similar or dissimilar methodology now known or hereafter developed.

The use of general descriptive names, registered names, trademarks, service marks, etc. in this publication does not imply, even in the absence of a specific statement, that such names are exempt from the relevant protective laws and regulations and therefore free for general use.

The publisher, the authors and the editors are safe to assume that the advice and information in this book are believed to be true and accurate at the date of publication. Neither the publisher nor the authors or the editors give a warranty, expressed or implied, with respect to the material contained herein or for any errors or omissions that may have been made. The publisher remains neutral with regard to jurisdictional claims in published maps and institutional affiliations.

This Springer imprint is published by the registered company Springer Nature Singapore Pte Ltd. The registered company address is: 152 Beach Road, #21-01/04 Gateway East, Singapore 189721, Singapore

*We are honored to dedicate the proceedings
of ICCVBIC 2021 to all the participants and
editors of ICCVBIC 2021.*

Preface

This conference proceedings volume contains the written versions of most of the contributions presented during the conference of ICCVBIC 2021. This conference provided a setting for discussing the recent developments in a wide variety of topics including computational vision, fuzzy, image processing and bio-inspired computing. This conference has been a good opportunity for participants coming from various destinations to present and discuss topics in their respective research areas.

ICCVBIC 2021 conference tends to collect the latest research results and applications on computational vision and bio-inspired computing. It includes a selection of 63 papers from 252 papers submitted to the conference from universities and industries all over the world. All of the accepted papers were subjected to strict peer-reviewing by 2–4 expert referees. The papers have been selected for this volume because of quality and the relevance to the conference.

ICCVBIC 2021 would like to express our sincere appreciation to all authors for their contributions to this book. We would like to extend our thanks to all the referees for their constructive comments on all papers, and especially, we would like to thank the organizing committee for their hard working. Finally, we would like to thank the Springer publications for producing this volume.

Coimbatore, India
Porto, Portugal
Arad, Romania

Dr. S. Smys
Dr. João Manuel R. S. Tavares
Dr. Valentina Emilia Balas

Acknowledgements

We would like to acknowledge the excellent work of our conference organising committee and keynote speakers for their presentations on November 25–26, 2021. The organizers also wish to acknowledge publicly the valuable services provided by the reviewers.

On behalf of the editors, organizers, authors and readers of this conference, we wish to thank the keynote speakers and the reviewers for their time, hard work and dedication to this conference. The organizers also wish to acknowledge speakers and participants who attended this conference. Many thanks for all persons who helped and supported this conference. ICCVBIC 2021 would like to acknowledge the contribution made to the organization by its many volunteers. Members contributed their time, energy and knowledge at a local, regional and international level.

We also thank all the chairpersons and conference committee members for their support.

Contents

Molecular Docking Analysis of Selected Phytochemicals for the Treatment of Proteus Syndrome	1
Tanwar Reeya and Das Asmita	
A Deep Learning-Based Detection of Wrinkles on Skin	25
H. Deepa, S. Gowrishankar, and A. Veena	
Image Transmission Using Leach and Security Using RSA in Wireless Sensor Networks	39
S. Aruna Deepthi, V. Aruna, and R. Leelavathi	
Code Injection Prevention in Content Management Systems Using Machine Learning	53
C. Kavithamani, R. S. Sankara Subramanian, Srinivasan Krishnamurthy, Jayakrishnan Chathu, and Gayatri Iyer	
A Review of Hyperspectral Image Classification with Various Segmentation Approaches Based on Labelled Samples	69
Sneha and Ajay Kaul	
Improvements in User Targeted Offline Advertising Using CNN and Deviation-Based Queue Scheduling	93
Ruchika Malhotra, Samarth Gupta, Sarthak Katyal, and Ronak Sakhuja	
Movie Recommendation System Using Hybrid Collaborative Filtering Model	109
Rohit Kale, Saurabh Rudrawar, and Nikhil Agrawal	
Hybrid Pipeline Infinity Laplacian Plus Convolutional Stage Applied to Depth Completion	119
Vanel Lazcano and Felipe Calderero	
A Novel Approach of DEMOO with SLA Algorithm to Predict Protein Interactions	135
P. Lakshmi and D. Ramyachitra	

Economic Load Dispatch Problem with Valve-Point Loading Effect Using DNLP Optimization Using GAMS 149
P. Dinakara Prasad Reddy, Ch. Devisree, M. Vijaya Kumar Naik, and K. Guna Prasad

Solar Radio Spectrum Classification Based on ConvLSTM 161
Ruru Cheng and Guowu Yuan

Particle Swarm Optimization-Based Neural Network for Wireless Heterogeneous Networks 173
Divya Y. Chirayil

Impact Analysis of COVID-19 on Various Indian Sectors 181
Shreya Nayak, Govind Thakur, and Narendra Shekoker

Emotion Recognition in Speech Using MFCC and Classifiers 197
G. Ajitha, Addagatla Prashanth, Chelle Radhika, and Kancharapu Chaitanya

A Comparative Analysis on Image Caption Generator Using Deep Learning Architecture—ResNet and VGG16 209
V. Sri Neha, B. Nikhila, K. Deepika, and T. Subetha

Corona Warrior Smart Band 219
Soham S. Methul, Shubhangee K. Varma, and Ashok S. Chandak

Cellular Learning Automata: Review and Future Trend 229
Mohammad Khanjary

Computer Vision and Machine Learning-Based Techniques for Detecting the Safety Violations of COVID-19 Scenarios: A Review 239
K. S. Kavitha and Megha P.Arakeri

Stigmergy-Based Collision-Avoidance Algorithm for Self-Organising Swarms 253
Paolo Grasso and Mauro Sebastián Innocente

Handling Security Issues in Software-defined Networks (SDNs) Using Machine Learning 263
Deepak Kumar and Jawahar Thakur

Multi-purpose Web Application Honeypot to Detect Multiple Types of Attacks and Expose the Attacker’s Identity 279
P. Sri Latha and S. Prasanth Vaidya

An Empirical Approach for Tuning an Autonomous Mobile Robot in Gazebo 289
Naveen Bharathiraman, Adwait Kaundanya, Jaiesh Singhal, Yash Wadalkar, and Kiran Talele

An Investigation on Computational Intelligent Solutions for Highly Dynamic Wireless Sensor Networks 301
 R. Haripriya, C. B. Vinutha, and M. Nagaraja

A Study of Underwater Image Pre-processing and Techniques 313
 Pooja Prasenana and C. D. Suriyakala

Multilabel Text Classification of Scientific Abstract 335
 T. R. Srinivas, A. V. S. Rithvik, and Saswati Mukherjee

Spirochaeta Bacteria Detection Using an Effective Semantic Segmentation Technique 355
 Apeksha Kulkarni, P. Sai Dinesh Reddy, Rishabh Bassi, Suryakant Kumar Kashyap, and M. Vijayalakshmi

An IoT-Based Intelligent Air Quality Monitoring System 367
 K. R. Chetan

Machine Learning-Based Sentiment Analysis Towards Indian Ministry 381
 K. Bhargavi, Pratish Mashankar, Pamidimukkala Vasista Sreevarsh, Radhika Bilolikar, and Preethi Ranganathan

Detection and Prediction for Obstructive Sleep Apnea Recognition 393
 T. Srinivas Reddy, A. Pradeep Kumar, M. Mahesh, and J. Prabhakar

A Comprehensive Study of Advances in Oral Cancer Detection Using Image Processing Techniques 401
 S. M. Sagari and Vindhya P. Malagi

Training a Multilayer Perception for Modeling Stock Price Index Predictions Using Modified Whale Optimization Algorithm 415
 Nebojsa Bacanin, Miodrag Zivkovic, Luka Jovanovic, Milica Ivanovic, and Tarik A. Rashid

Energy Saving Mechanism Using Extensive Game Theory Technique in Wireless Body Area Network (ES-EG) 431
 M. Ayesha Nasreen and Selvi Ravindran

Performance Analysis of Routing Methods for Unmanned Aerial Vehicle Network 449
 Supriya Kamble and Sanjay Pardeshi

Study of Classification Algorithms for Handwritten Character Recognition 461
 R. Sanjay Krishna, E. Jaya Suriya, and J. Shana

A Hybrid Multiclass Classifier Approach for the Detection of Malicious Domain Names Using RNN Model 471
 B. Aarthi, N. Jeenath Shafana, Judy Flavia, and Balika J. Chelliah

Brain Tumor Detection and Classification Using Transfer Learning Technique	483
Addepalli Venkatanand Ram, Harish Kuchulakanti, and Tarla Sai Raj	
A Comprehensive Survey of AI Methods to Predict Adverse Drug-Drug Interactions	495
P. Margaret Savitha and M. Pushpa Rani	
Feature Selection Using PSO Optimized-Framework with Machine Learning Classification System via Breast Cancer Survival Data	513
Anusha Papasani, Nagaraju Devarakonda, Zdzislaw Polkowski, Madhavi Thotakura, and N. Bhagya Lakshmi	
Inception-Based CNN for Low-Light Image Enhancement	533
Moomal Panwar and Sanjay B. C. Gaur	
Quantum Grid: Toward Future Energy Transformation	547
N. Samanvita, Sowmya Raman, Shruti Gatade, Anil Kumar, and Shreeram Kulkarni	
Computer Vision in Autoimmune Diseases Diagnosis—Current Status and Perspectives	571
Viktoria N. Tsakalidou, Pavlina Mitsou, and George A. Papakostas	
Covariance Features Improve Low-Resource Reservoir Computing Performance in Multivariate Time Series Classification	587
Sofía Lawrie, Rubén Moreno-Bote, and Matthieu Gilson	
Wireless Sensor-Based Enhanced Security Protocol to Prevent Node Cloning Attack	603
S. Meganathan, N. Rajesh Kumar, S. Sheik Mohideen Shah, A. Sumathi, and S. Santhoshkumar	
A Deep Convolutional Neural Network-Based Speech-to-Text Conversion for Multilingual Languages	617
S. Venkatasubramanian and R. Mohankumar	
A Novel Dual Model Approach for Categorization of Unbalanced Skin Lesion Image Classes	635
Shrey Dedhia, Siddharth Trivedi, Siddharth Salvi, Jay Jani, and Lynette D’mello	
A Study of Green Information Technology Using the Bibliometric Analysis	651
Agung Purnomo, Evaristus Didik Madyatmadja, Albert Verasius Dian Sano, Hendro Nindito, and Corinthias P. M. Sianipar	

Node Sleep Strategy for Improvement of Energy Efficiency in Wireless Multimedia Sensor Networks 667
 Minaxi Doorwar and P. Malathi

Analysis of Greenness in Urban Cities Using Supervised and Unsupervised Classification 675
 Nita Nimbarte, Shraddha Sainis, and Sanjay Balamwar

Sequence Models for Crop Yield Prediction Using Satellite Imagery 687
 M. Sarith Divakar, M. Sudheep Elayidom, and R. Rajesh

A Comparative Study of Word Embedding Techniques in Natural Language Processing 701
 Syed Abdul Basit Andrabi and Abdul Wahid

A Taxonomy on Strategic Viewpoint and Insight Towards Multi-Cloud Environments 713
 S. Alangaram and S. P. Balakannan

Instant Recipe Generation from Food Images 721
 Amogh Rajesh Desai, Sakshi Goel, Tanvi Karenavar, and Preet Kanwal

Breast Cancer Diagnosis Using Quantum-Inspired Classifier 737
 S. R. Sannasi Chakravarthy and Harikumar Rajaguru

Predictive Analysis Model for Mental Health 749
 Fazal Rehman, M. Lakshmi, K. Aditya Shastry, Syed Ismail, and Wasif Irshad

Detection and Counting of Fruit from UAV RGB Images Using Computer Vision 761
 Adel Mokrane, Abenasser Kadouci, Amal Choukchou-Braham, and Brahim Cherki

Efficient Segmentation of Tumor and Edema MR Images Using Optimized FFNN Algorithm 779
 Rehna Kalam and M. Abdul Rahiman

A Survey on Brain Computer Interface: A Computing Intelligence 795
 A. Shanmugapriya and A. Grace Selvarani

A Survey on Security and Privacy in Social Networks 807
 B. Jayaram and C. Jayakumar

A Novel Video Reconstruction of Randomized Frames Using ORB Descriptor 823
 M. Rohith, P. Priyanka, M. Kamalakar, and T. Kavitha

Prediction of the Wind Turbine Performances Using BEM Model Coupled to CFD Method 837
 Samah Laalej, Abdelfattah Bouatem, Ahmed Al Mers, and Rabii Elmaani

Development of Novel Face Recognition Techniques for VGG Model by Using Deep Learning 849
A. Arunraja, V. Mahendran, C. Mukesh, and M. Mahinesh

Enhanced Deep Hierarchical Classification Model for Smart Home-Based Alzheimer Disease Detection 863
C. Dhanusha and A. V. Senthil Kumar

SSO: A Hybrid Swarm Intelligence Optimization Algorithm 879
Arjun Nelikanti, G. Venkata Rami Reddy, and G. Karuna

Author Index 891

About the Editors

Dr. S. Smys received his M.E. and Ph.D. degrees all in Wireless Communication and Networking from Anna University and Karunya University, India. His main area of research activity is localization and routing architecture in wireless networks. He serves as Associate Editor of *Computers and Electrical Engineering (C&EE) Journal*, Elsevier and Guest Editor of *MONET Journal*, Springer. He is serving as Reviewer for *IET*, Springer, Inderscience and Elsevier journals. He has published many research articles in refereed journals and IEEE conferences. He has been General Chair, Session Chair, TPC Chair and Panelist in several conferences. He is Member of IEEE and Senior Member of IACSIT wireless research group. He has been serving as Organizing Chair and Program Chair of several International conferences, and in the Program Committees of several International conferences. Currently, he is working as professor in the Department of Information Technology at RVS technical Campus, Coimbatore, India.

João Manuel R. S. Tavares graduated in Mechanical Engineering at the Universidade do Porto, Portugal, in 1992. He also earned his M.Sc. degree and Ph.D. degree in Electrical and Computer Engineering from the Universidade do Porto in 1995 and 2001 and attained his Habilitation in Mechanical Engineering in 2015. He is Senior Researcher at the Instituto de Ciência e Inovação em Engenharia Mecânica e Engenharia Industrial (INEGI) and Associate Professor at the Department of Mechanical Engineering (DEMec) of the Faculdade de Engenharia da Universidade do Porto (FEUP). João Tavares is Co-Editor of more than 60 books, Co-Author of more than 50 book chapters, 650 articles in international and national journals and conferences and 3 international and 3 national patents. He has been Committee Member of several international and national journals and conferences, is Co-founder and Co-editor of the book series “Lecture Notes in Computational Vision and Biomechanics” published by Springer, Founder and Editor-in-Chief of the journal *Computer Methods in Biomechanics and Biomedical Engineering: Imaging and Visualization* published by Taylor & Francis, Editor-in-Chief of the journal *Computer Methods in Biomechanics and Biomedical Engineering* published by Taylor & Francis and Co-Founder and Co-chair of the international conference series: CompIMAGE, ECCOMAS

VipIMAGE, ICCEBS and BioDental. Additionally, he has been (Co-)Supervisor of several M.Sc. and Ph.D. thesis and Supervisor of several post-doc projects and has participated in many scientific projects both as Researcher and as Scientific Coordinator. His main research areas include computational vision, medical imaging, computational mechanics, scientific visualization, human–computer interaction and new product development.

Dr. Valentina Emilia Balas is currently Full Professor at “Aurel Vlaicu” University of Arad, Romania. She is Author of more than 300 research papers. Her research interests are in intelligent systems, fuzzy control and soft computing. She is Editor-in-Chief to *International Journal of Advanced Intelligence Paradigms* (IJAIP) and to *IJCSE*. Dr. Balas is Member of EUSFLAT, ACM and a SM IEEE, Member in TC—EC and TC-FS (IEEE CIS), TC—SC (IEEE SMCS) and Joint Secretary FIM.

Molecular Docking Analysis of Selected Phytochemicals for the Treatment of Proteus Syndrome



Tanwar Reeya and Das Asmita

Abstract Proteus syndrome is a rare hamartomatous disorder that is characterized by the overgrowth of tissues in a mosaic manner. Since drug therapy was not seen to be a component of standard care for Proteus syndrome, this paper focuses on finding phytochemicals against AKT-1 protein whose mutation is responsible for Proteus syndrome. Lipinski's rule of 5 was applied to check the drug-likeness of the selected phytochemicals followed by 3 rounds of molecular docking, computation of bioavailability radar and MD simulations. Simulations revealed Tanshinone-II A to be a potent inhibitor of AKT-1. Further, in-vivo studies can be performed on Tanshinone-II A for clinical use of the compound. In the above study, Miransertib (ARQ 092) was used as a positive control since it has recently shown to have a therapeutic effect on a teenager with Proteus syndrome and ovarian carcinoma.

Keywords Proteus syndrome · Molecular docking · AKT-1 · Miransertib · Phytochemicals

1 Introduction

Proteus syndrome is a rare disorder which involves an atypical skeletal growth [1]. This disease was first reported in the year 1979 followed by similar reports in the year 1983 by Wiedemann et al. It begins postnatally and progresses in a rapid and disproportionate manner which usually results in the distortion of the normal tissue [2]. There are cases in which many affected individuals are born without any perceptible symptoms, and the overgrowth usually begins during the time frame of 6–18 months. The severity and extent to which this disease can affect a patient vary greatly from one to another, but a few common manifestations of this disease are asymmetric,

T. Reeya (✉) · D. Asmita
Department of Biotechnology, Delhi Technological University, Main Bawana Road, Delhi
110042, India

D. Asmita
e-mail: asmitadas1710@dce.ac.in

distorting bony overgrowth, CCTN or cerebriform connective tissue nevi, dysregulation of fatty tissue and vascular anomalies [3]. The patients affected by this disease are susceptible to mesothelioma, breast cancer and papillary thyroid carcinoma since they have predisposition to benign and malignant tumours [4]. Although the exact cause of Proteus syndrome is not very clear, it has been seen that mutations in the AKT-1 gene that occurs after fertilization of the embryo (somatic mutation) are an important cause. AKT-1 is a part of the PI3K/AKT signalling pathway which is responsible for the regulation of various cellular processes such as the cell growth, proliferation and apoptosis [5]. The activation of AKT takes place due to its PH domain's interaction with a lipid or a secondary messenger called the phosphatidylinositol 3,4,5-trisphosphate [PI (3,4,5) P3]. Following this interaction, AKT-1 is then phosphorylated at threonine 308 (T308) by phosphoinositide-dependent kinase which also binds to [PI (3,4,5) P3]. AKT is fully activated when it is phosphorylated by mTORC2 complex at position 473 (Serine 473) [6]. Since bioinformatics helps in the reduction of cost of designing experiments, their execution and laboratory trials, we use it with the aim to produce results which would help us bring about the use of phytocompounds extracted from plants like *Sanguinaria canadensis*, *Evodia rutaecarpa*, *Salvia miltiorrhizae*, *Trigonella foenum*, etc. These plants have been selected due to their ability to participate in targeted therapeutic activity against AKT-1 protein in cancer. Miransertib has been used as a positive control for conducting molecular docking studies since the use of Miransertib (ARQ 092) has recently shown to have a therapeutic effect on a teenager with Proteus syndrome and ovarian carcinoma in 2019 [7]. Miransertib is an allosteric inhibitor of our target protein AKT-1 which binds to the combined interface of PH domain and the N and C lobe of kinase domain (Fig. 1). This binding enables the target protein to be locked in a closed conformation which results in the blocking of the phospholipid binding site by the kinase domain. The consequence of this conformation enables the allosterically inhibited AKT-1 to remain cytosolic and inactivated (activation occurs through phosphorylation) (Fig. 2). The nature of inhibition of Miransertib poses an advantage since a

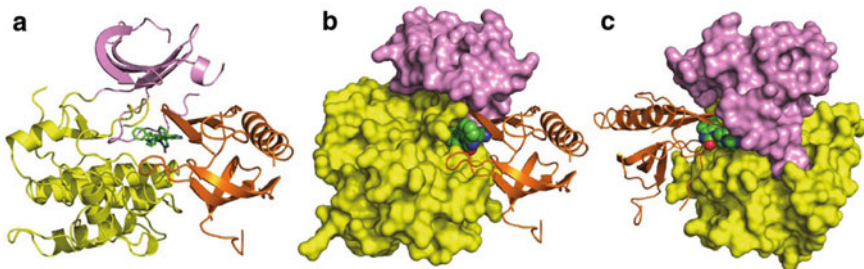


Fig. 1 a The following figure represents the orientation of the PH domain (orange) relative to the N-lobe (pink) and C-lobe (yellow) of the kinase domain and Inhibitor VIII shown in green. b In the same orientation as Panel A, the kinase domain is surface rendered. c Structure of AKT1(1–443): Inhibitor VIII rotated approximately 180° compared to Panel B. Courtesy: <https://doi.org/10.1371/journal.pone.0012913.g003> [8]

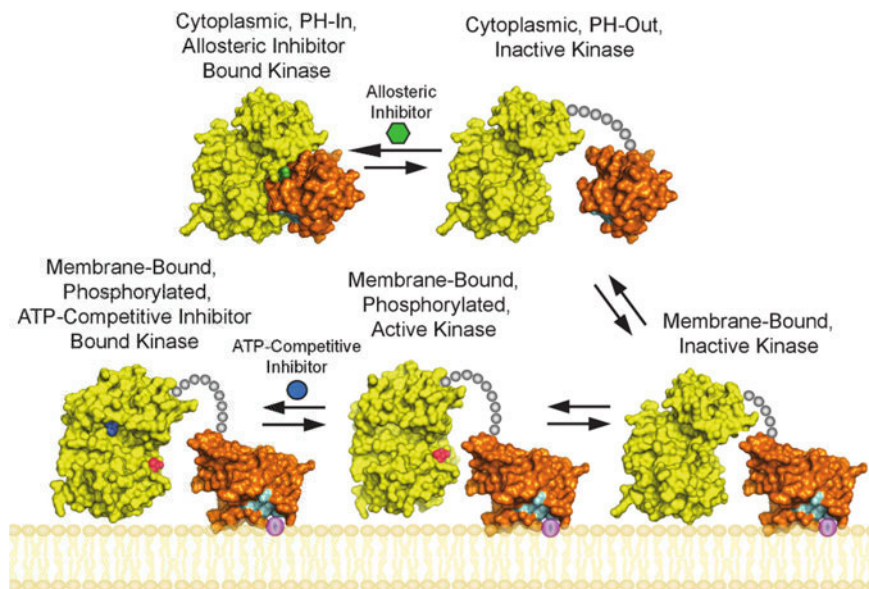


Fig. 2 Model of AKT activation and inhibition. In the cytoplasm, the ‘PH-in’ and ‘PH-out’ conformations of AKT are in equilibrium. AKT is recruited to the plasma membrane via interactions with the products of PI3K and is subsequently phosphorylated on two sites, T308 and S473 in AKT1, which results in kinase activation. The allosteric inhibitor stabilizes the ‘PH-in’ form of the inactive enzyme (top left); whereas the ATP-competitive inhibitor binds to the activated form of the kinase (bottom left). Surface representations derived from the following structures: PDB code: 3CQW (active and ATP-competitive inhibitor bound kinase), PDB code: 1UNQ (membrane-bound PH domain) and PDB code: 3O96 (cytoplasmic PH and kinase domains and membrane-bound kinase domain). Colouring as follows: kinase domain (yellow), PH domain (orange), IP4 binding residues (cyan), phospho-T308 (red), allosteric inhibitor (green), ATP-competitive inhibitor (blue) and PI3K products (violet). Phospho-S473 is not visible in these orientations of AKT. Courtesy: <https://doi.org/10.1371/journal.pone.0012913.g003> [8]

study conducted by Wu et al. in 2010 [8] hypothesized allosteric inhibitors to have a higher efficacy than small ATP-competitive molecules. They proposed this since the competitive inhibitor is not able to close the PH domain fully upon its binding due to which the kinase domain and the phospholipid binding site remain exposed [8]. This exposure enhances the ability of AKT to localize to the membrane, whereas the allosteric inhibitors restrict both membrane association and activation by phosphorylation. Although, a clinical perspective with respect to this observation is still needed [8]. Lastly, it is the first drug to go through clinical trials (Phase-II) in May, 2021 for Proteus syndrome. Hence, this research explores the properties of selected phytocompounds with respect to our target protein; AKT-1 keeping Miransertib as the positive control.

2 Methods and Materials

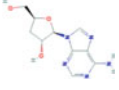
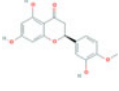
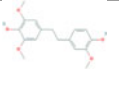
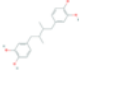
Building of Phytochemical Library: NPCARE (silver.sejong.ac.kr/npcancer/) or the Natural Products CARE is a database built by the Department of Bioscience and Biotechnology, Sejong University, consisting of a list of natural products that can regulate specific genes involved in cancer [9]. Each entry in this database is annotated with the name of genus and species of the biological source, the type of cancer it is involved with, the name of the cell line used to determine its anti-cancerous property, its PubChem ID and lastly a myriad of information about the target gene/protein. Since our research focusses on down regulating the effects AKT-1 gene for the treatment of Proteus syndrome, a list of 21 phytochemicals were obtained for AKT-1. (as shown in Table 1).

Protein/macromolecule and Ligands: Protein Data Bank or PDB (<https://www.rcsb.org/>) is a database that contains three-dimensional structural information of large biological molecules such as nucleic acids and proteins [10]. Our target protein AKT-1 was retrieved from the following database by using the PDB ID:3O96 in.pdb format. The structure contained a single A chain with an amino acid length of 446 along with a Covalent-Allosteric AKT Inhibitor. The publicly accessible PubChem repository has served as a resource of chemical information to the scientific community since 2004 (<https://pubchem.ncbi.nlm.nih.gov/>), and it contains information regarding the chemical and physical properties of the substance along with its structural representation (2-D,3-D, etc.) [11]. Three-dimensional structures of the ligands were obtained from PubChem repository using their respective PubChem IDs obtained from NPCARE database in.sdf format followed by their conversion to.pdb format using Biovia Discovery Studio.

ADME Analysis: In order to begin the screening of ligands, ADME analysis was conducted by applying Lipinski's rule of 5 [12]. The factors involved (molecular weight (<500 Da), high lipophilicity (LogP <5), hydrogen bonds donors (<5) and hydrogen bond acceptors (<10)) in conducting the same were retrieved from PubChem repository. According to this analysis, any ligand that violates more than 2 of the above stated parameters will be debarred from further analysis.

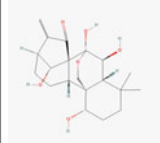
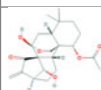
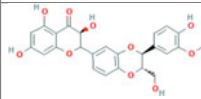
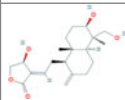
Molecular Docking Analysis: It is a regularly used computational tool which aids the process of designing drugs since it provides information regarding the binding mode of the known ligands, identification of potent drug candidates and their binding affinity. The following tool was used in three rounds to identify the binding affinity and the type of interactions our selected phytochemicals displayed. The first round of molecular docking was conducted by PyRx. It is an open-source (<https://pyrx.sourceforge.io/>) virtual screening tool which contains a combination of software's such as AutoDock Vina, AutoDock 4.2 and Open Babel [13]. For the following round of docking studies, AutoDock Vina tool compiled in PyRx was used. The dimensions used for this screening were centre (x, y, z) = (9.3494, -7.9442, 10.1538) and dimensions in angstrom (x, y, z) = (18.0256, 25.000, 24.4774). The water molecules and the allosteric inhibitor were removed beforehand. Lastly, an exhaustiveness of 8 was set to give the output of the lowest energy possible with the help of AutoDock

Table 1 ADME analysis of selected phytochemical

S.No.	Species	Compound name	PubChem ID	2-D diagram	ADME analysis
1	<i>Cordyceps militaris</i>	Cordycepin 3'-deoxyadenosine	CID 6303		Molecular weight (<500 Da) 251.24 g/mol Lipophilicity (LogP <5) – 1.94 H bond donor (<5) 3 H bond acceptor (<10) 6 Violations 0
2	Citrus spp.	Hesperetin	CID 72281		Molecular weight (<500 Da): 302.28 g/mol Lipophilicity (LogP <5): 0.41 H bond donor (<5): 3 H bond acceptor (<10): 6 Violations: 0
3	<i>Dendrobium loddigesii</i>	Moscaticolin	CID 176096		Molecular weight (<500 Da): 304.34 g/mol Lipophilicity (LogP <5): 1.94 H bond donor (<5): 2 H bond acceptor (<10): 5 Violations: 0
4	<i>Larrea divaricata</i>	Nordihydroguaiaretic acid	CID 4534		Molecular weight (<500 Da): 302.36 g/mol Lipophilicity (LogP <5): 2.74 H bond donor (<5): 4 H bond acceptor (<10): 4 Violations: 0

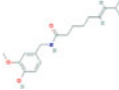
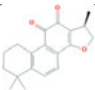


(continued)

Table 1 (continued)

S.No.	Species	Compound name	PubChem ID	2-D diagram	ADME analysis
5	Oridonin	Oridonin	CID 5321010		Molecular weight (<500 Da): 364.43 g/mol Lipophilicity (LogP <5): 0.86 H bond donor (<5): 4 H bond acceptor (<10): 6 Violations: 0
6	Rabdosia coetsa	Rabdoceosin B	CID 10452999		Molecular weight (<500 Da): 390.47 g/mol Lipophilicity (LogP <5): 2.01 H bond donor (<5): 2 H bond acceptor (<10): 6 Violations: 0
7	Silybum marianum	Silibinin	CID 16211710		Molecular weight (<500 Da): 482.44 g/mol Lipophilicity (LogP <5): -0.40 H bond donor (<5): 5 H bond acceptor (<10): 10 Violations: 0
8	Andrographis paniculata	Andrographolide	CID 5318517		Molecular weight (<500 Da): 350.45 g/mol Lipophilicity (LogP <5): 1.98 H bond donor (<5): 3 H bond acceptor (<10): 5 Violations: 0

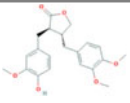
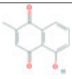

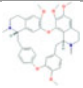
(continued)

Table 1 (continued)

S.No.	Species	Compound name	PubChem ID	2-D diagram	ADME analysis
9	Capsicum spp.	Capsaicin	CID 1548943		Molecular weight (<500 Da): 305.41 g/mol Lipophilicity (LogP <5): 2.69 H bond donor (<5): 2 H bond acceptor (<10): 3 Violations: 0
10	Salvia miltiorrhizae	Cryptotanshinone	CID 160254		Molecular weight (<500 Da): 296.36 g/mol Lipophilicity (LogP <5): 2.36 H bond donor (<5): 0 H bond acceptor (<10): 3 Violations: 0
11	Allium sativum	Diallyl trisulfide	CID 16315		Molecular weight (<500 Da): 178.34 g/mol Lipophilicity (LogP <5): 2.35 H bond donor (<5): 0 H bond acceptor (<10): 0 Violations: 0
12	Isaria sinclairii	FTY720	CID 107969		Molecular weight (<500 Da): 343.93 g/mol Lipophilicity (LogP <5): 3.24 H bond donor (<5): 3 H bond acceptor (<10): 3 Violations: 0

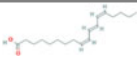
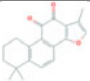
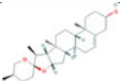
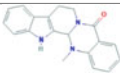
(continued)

Table 1 (continued)

S.No.	Species	Compound name	PubChem ID	2-D diagram	ADME analysis
13	Arctium lappa	Arctigenin	CID 64981		Molecular weight (<500 Da): 372.41 g/mol Lipophilicity (LogP <5): 2.12 H bond donor (<5): 1 H bond acceptor (<10): 6 Violations: 0
14	Plumbago zeylanica	Plumbagin	CID 10205		Molecular weight (<500 Da): 188.18 g/mol Lipophilicity (LogP <5): 0.59 H bond donor (<5): 1 H bond acceptor (<10): 3 Violations: 0
15	Pterocarpus marsupium	Pterostilbene	CID 5281727		Molecular weight (<500 Da): 256.30 g/mol Lipophilicity (LogP <5): 2.76 H bond donor (<5): 1 H bond acceptor (<10): 3 Violations: 0
16	Stephania tetrandra	Tetrandrine	CID 73078		Molecular weight (<500 Da): 622.75 g/mol Lipophilicity (LogP <5): 3.73 H bond donor (<5): 0 H bond acceptor (<10): 8 Violations: 1


(continued)

Table 1 (continued)

S.No.	Species	Compound name	PubChem ID	2-D diagram	ADME analysis
17	<i>Punica granatum</i>	Punicic_acid	CID 5281126		Molecular weight (<500 Da): 278.43 g/mol Lipophilicity (LogP <5): 4.38 H bond donor (<5): 1 H bond acceptor (<10): 2 Violations: 0
18	<i>Salvia miltiorrhizae</i>	Tanshinone-IIA	CID 164676		Molecular weight (<500 Da): 294.34 g/mol Lipophilicity (LogP <5): 2.24 H bond donor (<5): 0 H bond acceptor (<10): 3 Violations: 0
19	<i>Trigonella foenum</i>	Diosgenin	CID 99474		Molecular weight (<500 Da): 414.62 g/mol Lipophilicity (LogP <5): 4.94 H bond donor (<5): 1 H bond acceptor (<10): 3 Violations: 0
20	<i>Evodia rutaecarpa</i>	Isoevodiamine	CID 151289		Molecular weight (<500 Da): 303.36 g/mol Lipophilicity (LogP <5): 3.16 H bond donor (<5): 1 H bond acceptor (<10): 1 Violations: 0

(continued)

Table 1 (continued)

S.No.	Species	Compound name	PubChem ID	2-D diagram	ADME analysis
21	<i>Sanguinaria canadensis</i>	Sanguinarine	CID 5154		Molecular weight (<500 Da): 332.33 g/mol Lipophilicity (LogP <5): 2.72 H bond donor (<5): 0 H bond acceptor (<10): 4 Violations: 0

Vina-PyRx, and the ligands were then filtered out on the basis of their binding energy. The selected ligands were then docked further in two more rounds using another open-source docking tool, AutoDock 4.2 (<http://autodock.scripps.edu/>) [14]. Optimization of both the protein and the ligand was carried out by eliminating water, including polar hydrogens followed by adding Kollman and Gasteiger charges. The final step of optimization was carried out by removing the native ligand of the protein. The output utilized for docking studies with an exhaustiveness set to 10 was Lamarckian GA, and the best results out of the two were then used for further analysis.

Bioavailability Radar: SwissADME is an online tool (<http://www.swissadme.ch/>) which was used to obtain a bioavailability radar, and this radar scrutinized the phytochemicals on the basis of six parameters (saturation, flexibility, solubility, size, polarity and lipophilicity). The region coloured in pink defines the limit within which the parameters should lie, and any deviation from the region indicated that the drug is not orally bioavailable.

Molecular Dynamics: The docked complex was subjected to molecular dynamics simulation by the use of Demond-Maestro module [15]. Since the software provides high performance algorithms in its default settings itself, they were used to obtain high speed and precise results. The docked complex was subjected to submersion in TIP3P water model in an orthorhombic shape, after which the entire system was neutralized by addition of seven chlorine ions at 0.15 M concentration. All the atoms in the system were aligned by optimized potentials for liquid simulations-AA (OPLS-AA) 2005 force field. SHAKE/RATTLE algorithm along with NVT as the ensemble class was used to limit the movement of the atoms covalently bonded. The conditions set in order to start the simulations were temperature: 300 K and pressure: 1 bar for 100 ns. Integration of all the parameters of dynamic simulation was carried out using the RESPA integrator. Finally, to analyse the component stability and dynamic nature of interaction, a trajectory of 100 ns was set to show in 1000 frames.

3 Results and Discussion

ADME Analysis: 21 compounds were screened with respect to Lipinski's rule of 5, and the parameters used for the same were molecular weight (<500 Da), hydrogen bonds donors (<5), high lipophilicity (LogP <5) and hydrogen bond acceptors (<10). This screening helped in determining the drug-likeness of the selected phytochemicals. Usually, compounds are eliminated if they violate more than two parameters of Lipinski's rule of five. Out of the 21 compounds, 20 showed 0 violations leaving Tetrandrine with PubChem ID: 73078 with one violation (due to its molecular weight being greater than 500) as shown in Table 1.

Since all 21 of them fell within the parameters, it helped us conclude that all 21 compounds do not show any poor absorption or permeation, and hence, they were all used for further investigation.

Docking Analysis: The 21 selected phytochemicals were then introduced into a virtual space to conduct molecular docking studies. This was conducted in three rounds, first being conducted by PyRx and the last two by AutoDock 4.2. The active site residues for AKT-1 were obtained from a research study of the crystal structure of AKT-1 protein with an allosteric inhibitor by Wen-I Wu et al. in [8]. The residues at the active site of AKT-1 were VAL201, SER205, VAL270, THR82, CYS296, VAL83, GLU85, ILE84, ARG273, ASN54, ASP274, VAL271, TYR272, THR211, THR291, ILE290, ASP292, LEU210, LEU264, TRP80 and LYS268. These active sites are present at the linkage of PH domain and the N and C lobe of kinase domain.

Docking Analysis using AutoDock Vina-PyRx: The first round of docking analysis was conducted to identify the phytochemicals that have the ability to compete with Miransertib as a potent inhibitor by comparing their resultant vina binding affinities. As depicted by Table 2, results obtained by PyRx revealed that the binding energies of Diosgenin (−12.6 kcal/mol), Sanguinarine (−12.2 kcal/mol) and Tanshinone-IIA (−11.7 kcal/mol) are to be greater than that of Miransertib (−11.6 kcal/mol) which was taken as a positive control due to its therapeutic properties. Due to their depiction of greater binding strength than the positive control, these three phytochemicals, Disogenin, Sanguinarine and Tanshinone-IIA, were then selected for further docking.

Docking Analysis using AutoDock 4.2: The three phytochemicals, namely Disogenin, Tanshinone-II and Sanguinarine, were selected for two more rounds of molecular docking studies which were conducted by Autodock 4.2. The residues used for this round were the same as mentioned above.

The value of the best confirmation of Disogenin out of the 20 obtained was seen to be −11.39 kcal/mol. The four different types of interactions observed were pi-alkyl conventional hydrogen bond, van der Waals, and alkyl, and TRP80, LEU210, LEU264 and VAL270 were seen to be interacting via alkyl and pi-alkyl bond while LYS268, THR211 were seen to be interacting via conventional hydrogen bond, respectively. The remaining residues weakly interacted with the ligand via van der Waals interaction. (Fig. 1).

Table 2 Molecular docking results of 20 compounds with 3O96 using AutoDock Vina tool compiled in PyRx

S. No.	Compound name	Vina binding affinity (kcal/mol)
1	Cordycepin 3'-deoxyadenosine	-7.7
2	Hesperetin	-9.6
3	Moscatilin	-8.4
4	Nordihydroguaiaretic acid	-9.4
5	Oridonin	-8.6
6	Rabdocoetsin B	-8.5
7	Silibinin	-7.7
8	Andrographolide	-9.9
9	Capsaicin	-8.2
10	Cryptotanshinone	-11.6
11	Diallyl trisulfide	-4.1
12	FTY720	-7.8
13	Arctigenin	-10.1
14	Plumbagin	-7.9
15	Pterostilbene	-8.4
16	Tetrandrine	-6.3
17	Punicic_acid	-7.2
18	Tanshinone-IIA	-11.7
19	Diosgenin	-12.6
20	Isoevodiamine	-9.2
21	Sanguinarine	-12.2
22	Miransertib (Positive Control)	-11.6

The value of the best confirmation of Sanguinarine out of the 20 obtained was seen to be -9.57 kcal/mol. A total of eight interactions were observed including van der Waals, alkyl, pi-alkyl, conventional hydrogen bond, pi-sigma, pi-pi stacked, pi-anion and carbon hydrogen bond. LEU 264 was seen to be interacting via pi-stigma bond, TRP80 was seen to be interacting via pi-pi stacked bond, LEU210, VAL270 were seen to be interacting via alkyl and pi-alkyl bond, ASP 292 was seen to be interacting via pi-anion bond, ILE 290 was seen to be interacting via carbon hydrogen bond, lastly LYS268 and SER 205 were seen to be interacting via conventional hydrogen bond, and the rest weakly interacted with the ligand via van der Waals interaction. (Fig. 2).

The value of the best confirmation of Tanshinone-IIA out of the 20 obtained was seen to be -9.19 kcal/mol. A total of six interactions were observed including van der Waals, alkyl, pi-alkyl, conventional hydrogen bond, pi-sigma and pi-pi stacked.

VAL270 was seen to interacting via pi-sigma bond, TRP80 was seen to be interacting via pi-pi stacked, LEU210 and LEU264 were seen to be interacting via alkyl and pi-alkyl, lastly LYS268 was seen to be interacting via conventional hydrogen bond, and the rest weakly interacted with the ligand via van der Waals interaction. (Figs. 3 and 4).

Even though the three compounds displayed a lesser binding energy than that of our positive control they were further investigated since they had an added advantage of being derived from natural resources, we have further created the bioavailability

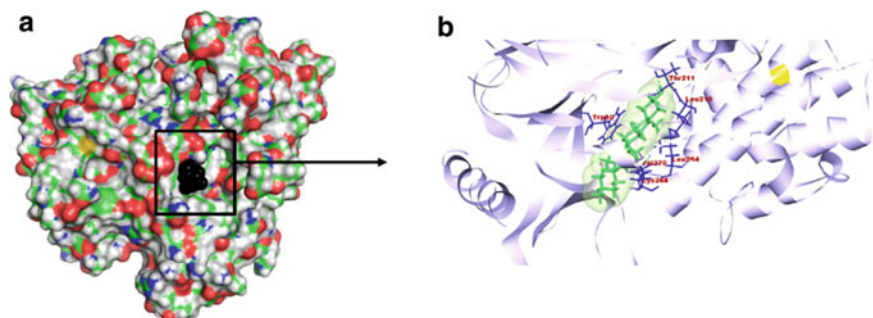


Fig. 3 Visualization of the docked complex Disogenin-3O96 **a** 3O96 is represented in the form of surface, and the ligand coloured in black is represented in the form of spheres illustrating the binding pocket. **b** A closer look at the interactions can be observed wherein the structure coloured in metallic purple represents the protein, the blue coloured sticks represent the protein groups, the green coloured ball and stick representation depicts the ligand: Disogenin, and the light green coloured surface around the ligand represents the binding pocket

Fig. 4 2-D interaction diagram of Disogenin

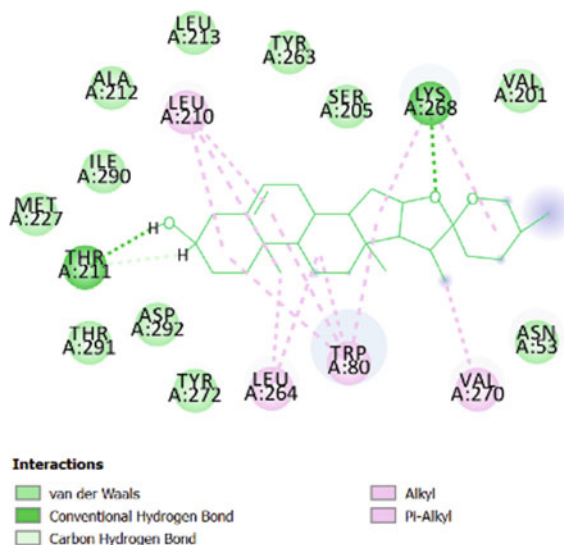


Table 3 Results based on different techniques

S. No.	Name	Binding energy (ΔG) (Kcal/mol)	Ligand efficiency	Inhibition constant (NM)	Intermolecular energy	Vdw H bond desolvation
1	Diosgenin	-11.39	-0.38	4.5	-11.69	-11.55
2	Tanshinone-IIA	-9.19	-0.37	182.78	-9.36	-9.11
3	Sanguinarine	-9.57	-0.44	97.04	-9.57	-9.29
4	Miransertib (positive control)	-11.47	-0.35	3.94	-13.25	-12.77

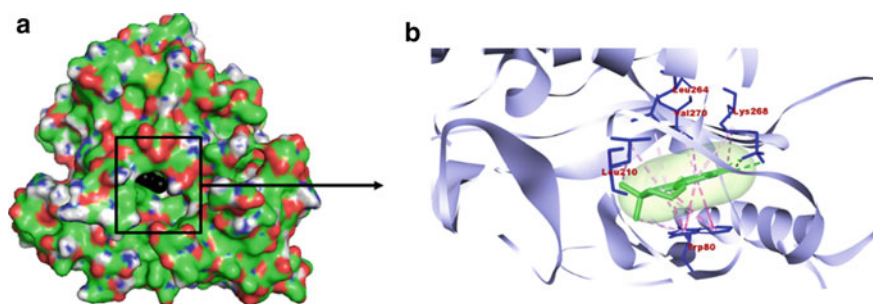


Fig. 5 Visualization of the docked complex Tanshinone-IIA-3O96 **a** 3O96 is represented in the form of surface, and the ligand coloured in black is represented in the form of spheres illustrating the binding pocket. **b** A closer look at the interactions can be observed wherein the structure coloured in metallic purple represents the protein, the blue coloured sticks represent the protein groups, the green coloured ball and stick representation depicts the ligand: Tanshinone-IIA, and the light green coloured surface around the ligands represents the binding pocket

radar and conducted molecular dynamics which is shown in Table 3 (Figs. 5, 6, 7 and 8).

Bioavailability Radar: The three selected compounds, Diosgenin, Tanshinone-II A and Sanguinarine, were then further investigated by computing the bioavailability radar, and this helped us in giving a closer look at the drug-likeness of the phyto-compound. The area in pink depicts the optimal range for each property; size: MW between 150 and 500 g/mol, lipophilicity: XLOGP3 between -0.7 and +5.0, solubility: log S not higher than 6, polarity: TPSA between 20 and 130 Å², saturation: fraction of carbons in the sp³ hybridization not less than 0.25, and flexibility: no more than nine rotatable bonds. This analysis found that Diosgenin and Tanshinone-IIA were both orally bioavailable. Sanguinarine on the other hand was not found to be orally bioavailable since it very clearly disobeyed the saturation parameter (Fig. 9).

Molecular Dynamics: The stability of the protein upon binding of a small molecule is the most integral property to be explored, and in order to do the same, the docked complexes of the two compounds: Diosgenin and Tanshinone-IIA were further subjected to molecular dynamics for 100 ns using Demond-Maestro